

# The University of Bradford Institutional Repository

<http://bradscholars.brad.ac.uk>

This work is made available online in accordance with publisher policies. Please refer to the repository record for this item and our Policy Document available from the repository home page for further information.

To see the final version of this work please visit the publisher's website. Access to the published online version may require a subscription.

**Link to publisher version:** <https://doi.org/10.1002/cnma.201800054>

**Citation:** Insua I, Petit M, Blackman LD et al (2018) Structural Determinants of the Stability of Enzyme-Responsive Polyion Complex Nanoparticles Targeting Pseudomonas aeruginosa's Elastase. ChemNanoMat. Accepted for publication.

**Copyright statement:** © 2018 The Authors. This is an Open Access article distributed under the [Creative Commons CC-BY license](#).

## Peptide Nanoparticles

# Structural Determinants of the Stability of Enzyme-Responsive Polyion Complex Nanoparticles Targeting *Pseudomonas aeruginosa*'s Elastase

Ignacio Insua,<sup>[a, b]</sup> Marion Petit,<sup>[a]</sup> Lewis D. Blackman,<sup>[c]</sup> Robert Keogh,<sup>[c]</sup> Anaïs Pitto-Barry,<sup>[c, e]</sup> Rachel K. O'Reilly,<sup>[c]</sup> Anna F. A. Peacock,<sup>[a]</sup> Anne Marie Krachler,<sup>[b, d]</sup> and Francisco Fernandez-Trillo<sup>\*[a, b]</sup>

**Abstract:** Here, we report how the stability of polyion complex (PIC) particles containing *Pseudomonas aeruginosa*'s elastase (LasB) degradable peptides and antimicrobial poly(ethylene imine) is significantly improved by careful design of the peptide component. Three LasB-degradable peptides are reported herein, all of them carrying the LasB-degradable sequence –GLA– and for which the number of anionic amino acids and cysteine units per peptide were systematically varied. Our results suggest that while net charge and potential to cross-link via disulfide bond formation do not have a predictable effect on the ability of LasB to degrade

these peptides, a significant effect of these two parameters on particle preparation and stability is observed. A range of techniques has been used to characterize these new materials and demonstrates that increasing the charge and cross-linking potential of the peptides results in PIC particles with better stability in physiological conditions and upon storage. These results highlight the importance of molecular design for the preparation of PIC particles and should underpin the future development of these materials for responsive drug delivery.

## Introduction

Polyion complex (PIC) (nano)particles, also known as polyelectrolyte complexes (PECs)<sup>[1]</sup> or interpolyelectrolyte complexes (IPECs),<sup>[2]</sup> are soft colloids obtained from the self-assembly of oppositely charged polyelectrolytes in solution.<sup>[3]</sup> These nanomaterials are attractive vehicles for the delivery of charged drugs such as antineoplastics,<sup>[4–7]</sup> antimicrobials<sup>[8–14]</sup> and nucleic

acids,<sup>[15]</sup> which can be complexed with oppositely charged polymers to form PIC (nano)particles that reduce the toxicity and/or control the activity of these drugs. Given the key role of enzymes in many diseases and their remarkable specificity,<sup>[16]</sup> PIC (nano)particles prepared from polyelectrolytes that degrade in the presence of these enzymes have a great potential for biomedical applications. This approach is particularly interesting to tackle infections, since many pathogens secrete enzymes (e.g. proteases) to overcome the host defenses.<sup>[17]</sup> By incorporating enzyme-responsive components into the PIC (nano)particle, the release of the antimicrobial can be localized to the surroundings of the pathogenic organism, leading to improved therapeutic profiles.

With these principles in mind, we have recently reported the preparation of enzyme-responsive PIC nanoparticles for the targeted delivery of antimicrobial branched poly(ethylene imine) (B-PEI), which was released upon exposure to *Pseudomonas aeruginosa*'s elastase LasB.<sup>[18]</sup> To this end, anionic peptide P1<sub>SH</sub> (Figure 1) was designed, that contained the amino acid sequence glycine-leucine-alanine (–GLA–), which is hydrolyzed by LasB. This sequence was inserted in between two glutamic acids (E), responsible for the electrostatic interaction with B-PEI, and two cysteines (C), to cross-link via disulfide formation once the nanoparticle is formed. The reported PIC nanoparticles showed excellent potential for the targeted delivery of B-PEI to *P. aeruginosa*, being specifically degraded by the bacterial elastase and displaying a LasB-specific activity against *P. aeruginosa*. However, the overall antimicrobial activity of the particles was low, with only 20% of the activity of free B-PEI

[a] Dr. I. Insua, M. Petit, Dr. A. F. A. Peacock, Dr. F. Fernandez-Trillo  
School of Chemistry  
University of Birmingham  
Edgbaston, B15 2TT, UK  
E-mail: f.fernandez-trillo@bham.ac.uk

[b] Dr. I. Insua, Dr. A. M. Krachler, Dr. F. Fernandez-Trillo  
Institute of Microbiology and Infection – School of Biosciences  
University of Birmingham  
Edgbaston, B15 2TT, UK

[c] Dr. L. D. Blackman, R. Keogh, Dr. A. Pitto-Barry, Prof. R. K. O'Reilly  
Department of Chemistry  
University of Warwick  
Coventry, CV4 7AL, UK

[d] Dr. A. M. Krachler  
Current address: Department of Microbiology and Molecular Genetics,  
University of Texas Health Science Center, Houston (TX), USA

[e] Dr. A. Pitto-Barry  
Current address: School of Chemistry and Biosciences, University of Bradford,  
Bradford BD7 1DP

Supporting information for this article is available on the WWW under  
<https://doi.org/10.1002/cnma.201800054>

© 2018 The Authors. Published by Wiley-VCH Verlag GmbH & Co. KGaA.  
This is an open access article under the terms of the Creative Commons  
Attribution License, which permits use, distribution and reproduction in any  
medium, provided the original work is properly cited.

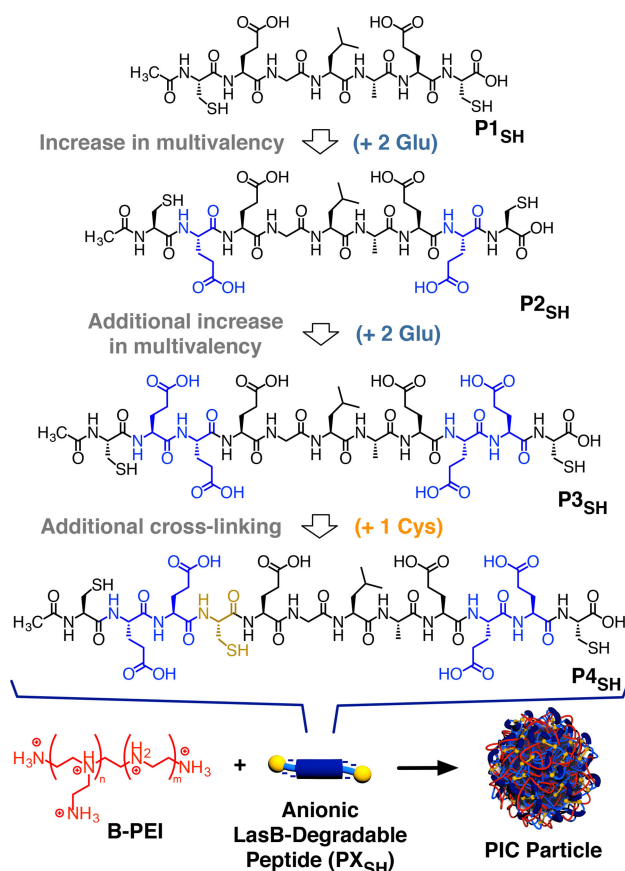


**Figure 1.** Structures of the LasB-degradable peptides evaluated in this work and their self-assembly with branched poly(ethylene imine) (B-PEI) to form antimicrobial PIC particles.

recovered in the presence of *P. aeruginosa*. Due to the low multivalency of peptide **P1<sub>SH</sub>**, only a small range of formulations resulted in the formation of stable PIC nanoparticles, thus compromising optimization of the delivery system.

In this article, we present our efforts to improve the stability of these LasB-responsive PIC particles by optimizing the structure of the peptide component. Three new LasB-responsive peptides were prepared with increasing number of anionic residues and cross-linking groups (Figure 1, **P2<sub>SH</sub>**–**P4<sub>SH</sub>**). The hydrolysis of peptides **P2<sub>SH</sub>**–**P4<sub>SH</sub>** by LasB was evaluated and compared to that caused by a model human elastase. While the extent and specificity of hydrolysis was influenced by their amino acid sequence, no clear correlation between multivalency and susceptibility to LasB was observed. When mixed with the antimicrobial B-PEI, all these peptides were able to give PIC particles across a wide range of formulations. Representative PIC particles were characterized using a range of light scattering techniques, suggesting that no significant structural differences could be observed between nanoparticles. Finally, the stability of these nanoparticles under simulated physiological conditions or under storage was also evaluated. Overall, particles prepared with the new peptides **P2<sub>SH</sub>**–**P4<sub>SH</sub>** showed better stability than those obtained from **P1<sub>SH</sub>**, with increasing stability in simulated physiological conditions as the multivalency of the peptides was increased.

## Results and Discussion

### Peptide Design and Synthesis

Based on the structure of LasB-responsive peptide **P1<sub>SH</sub>** (Ac-C-E-GLA-E-C-OH), previously reported by our group,<sup>[18]</sup> two modifications were proposed to enhance the saline stability of the resulting PIC nanoparticles: i) Additional glutamic acids were introduced to increase the number of anionic residues (Figure 1, **P2<sub>SH</sub>** and **P3<sub>SH</sub>**), potentially leading to a stronger affinity for antimicrobial B-PEI; and ii) the incorporation of a third cysteine (Figure 1, **P4<sub>SH</sub>**), which is expected to increase the cross-linking density via disulfide formation once the PIC nanoparticles are formed. Both charge density and cross-linking density have been reported as factors contributing to the stability of this type of nanoparticles.<sup>[3]</sup> Overall, the peptides prepared included either two additional glutamic acids (**P2<sub>SH</sub>**), four additional glutamic acids (**P3<sub>SH</sub>**), or four additional glutamic acids and an extra cysteine (**P4<sub>SH</sub>**) compared to the parent peptide **P1<sub>SH</sub>**. All peptides were synthesized by solid-phase chemistry in good to excellent yields and high purity without any chromatographic purification (see SI: Figures S1–S3† for experimental details and characterization).

### Enzymatic Degradation of Peptides

Next, the degradation of peptides **P1<sub>SH</sub>**–**P4<sub>SH</sub>** by *P. aeruginosa*'s elastase (LasB) was evaluated. This experiment involved quantification of the number of primary amines formed as a result of peptide hydrolysis, using the fluorescent reporter fluorescamine.<sup>[19]</sup> *P. aeruginosa*'s LasB hydrolyses peptides containing the –GLA– sequence between the glycine and leucine residues.<sup>[20]</sup> In these experiments, the fluorescent intensity of all fluorescamine adducts (Figure S4) was compared to that observed in the presence of H<sub>2</sub>N-LAE-OH (**P5**). **P5**'s sequence should be formed following LasB-mediated hydrolysis of the –GLAE– sequence, present in all the peptides reported. Thus, 100% hydrolysis was assigned to the fluorescent intensity of the fluorescamine adduct of **P5** and all other intensities reported as a percentage of this one (Figure 2). The degradation of peptides **P1<sub>SH</sub>**–**P4<sub>SH</sub>** in the presence of Human Leukocyte Elastase (HLE), a protease released by white blood cells during *P. aeruginosa* infections,<sup>[21]</sup> was also evaluated. This comparison allowed us to assess if these peptides were selectively hydrolyzed by the bacterial elastase over a relevant human enzyme.

All peptides were hydrolyzed by LasB, in agreement with our previous work that demonstrated that the addition of extra amino acids around the –GLA– tripeptide did not seriously compromise the activity of LasB.<sup>[18]</sup> We anticipated that increasing the number of glutamic acids could have a detrimental effect on the activity of LasB, due to the potential sequestration of Ca<sup>2+</sup> by carboxylic acids. Ca<sup>2+</sup> is a LasB cofactor and polycarboxylated compounds, in our case ethylenediaminetetraacetic acid (EDTA), are commonly used to quench the activity of the enzyme. However, no obvious trend was observed for our peptides. **P1<sub>SH</sub>**, **P3<sub>SH</sub>** and **P4<sub>SH</sub>** displayed

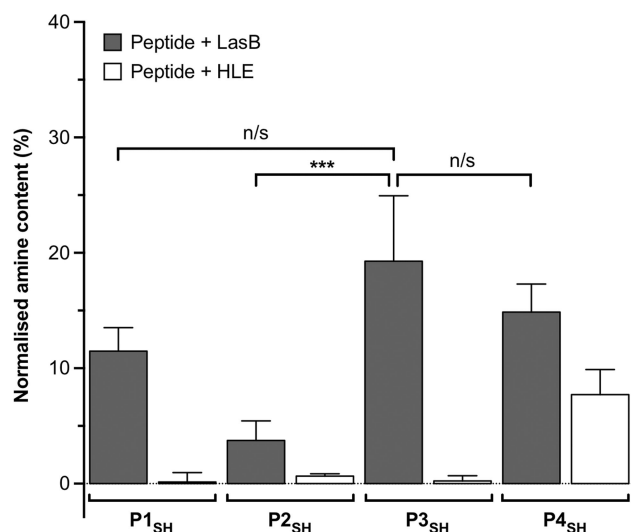


**Figure 2.** Relative amine content in samples of LasB responsive anionic peptides evaluated in this work. Relative amine content was calculated from fluorecamine conjugates formed following incubation with enzymes for 4 hours and normalized to the fluorescence observed with a model degradation peptide (P5, H<sub>2</sub>N-LA-E-OH) (Figure S4).  $n = 3$ , mean values  $\pm$  standard deviation. One-way ANOVA, followed by Tukey's test (CI = 95%) was used to test for significance. Statistical significance was determined 'n/s' = not significant, \*\*\*  $p < 0.001$ .

the highest susceptibility to LasB hydrolysis, with no statistical difference between them (Figure 2). Interestingly, P2<sub>SH</sub> was the least active of the peptides tested, despite having an intermediate number of glutamic acid residues. The potential of these peptides to adopt different conformations in solution that could explain this difference in activity was evaluated using circular dichroism (CD). However, CD suggested that all peptides had a random/extended conformation in solution without any significant difference across the collection (Figure S5A).<sup>[22]</sup> Finally, introducing an additional cysteine did not have a big effect on the activity of LasB, with the number of amines obtained from the hydrolysis of P4<sub>SH</sub> only 5% smaller than those obtained from P3<sub>SH</sub>. However, this extra cysteine had a significant effect on the specificity of the peptide with P4<sub>SH</sub> being the only peptide significantly degraded by HLE (ca. 50% of the hydrolysis observed with LasB, Figure 2). This loss of specificity is in agreement with the ability of HLE to cleave at cysteine residues,<sup>[23,24]</sup> while LasB's activity is moderately inhibited by thiols and cysteine residues.<sup>[25–27]</sup>

### Self-assembly and Characterization of PIC Particles

Having established that all peptides were hydrolyzed by LasB, we then explored their suitability for the preparation of B-PEI containing PIC nanoparticles. These nanoparticles were prepared by mixing peptides P1<sub>SH</sub>–P4<sub>SH</sub> with B-PEI in aqueous medium at physiological pH as previously reported for P1<sub>SH</sub>.<sup>[18]</sup> The colloidal stability of PIC particles is highly dependent on their charge ratio (i.e. the relative number of positive and negative charges mixed in the formulation). Therefore, several formulations were explored for each peptide, where the relative

number of cationic amines in B-PEI versus anionic carboxylic acids in peptides P1<sub>SH</sub>–P4<sub>SH</sub> (N:COOH ratio) was systematically varied (Figure 3, Table S1). From their  $\zeta$ -potentials, formulations of these LasB-responsive peptides could be split into 3 groups: a) *Formulations resulting in the formation of cationic nanoparticles*: While this was the case for all of the formulations made from P1<sub>SH</sub> (Figure 3, top), only those formulations with the smallest amounts of P2<sub>SH</sub>–P4<sub>SH</sub> peptides resulted in particles with a positively charged corona (Figure 3, 0.4 and 0.3 N:COOH ratios). b) *Formulations that yielded negatively charged nanoparticles*: We had previously reported that P1<sub>SH</sub> was unable to form negatively charged particles (Figure 3, top),<sup>[18]</sup> possibly because of its small size and multivalency. We were therefore very pleased to see that increasing the multivalency for P2<sub>SH</sub>–P4<sub>SH</sub> resulted in particles with a negatively charged corona for a broad range of formulations (Figure 3). This was particularly the case for P3<sub>SH</sub> and P4<sub>SH</sub>, the two peptides with the highest multivalency of the ones reported, which yielded negatively charged particles for formulations with N:COOH ratios  $\geq 0.6$ . c) *A region where no PIC nanoparticles formed* in agreement with the mechanism of nucleation for this type of supramolecular aggregates.<sup>[2,3,28]</sup> When mixed, polyelectrolytes will interact to form a neutral core made of a stoichiometric mixture of oppositely charged polyelectrolytes, surrounded by a corona of whichever polyion is present in excess. Neutral complexes that lack a charged stabilizing corona will not be colloiddally stable and flocculation of particles will occur. While this phenomenon was observed at 1:1 N:COOH ratios or above for P1<sub>SH</sub>,<sup>[18]</sup> unstable particles were formed at a 1:0.5 N:COOH ratio for all the new peptides. Interestingly, P2<sub>SH</sub> showed the smallest range of formulation that yielded colloiddally stable particles (Figure 3), suggesting again that this peptide may adopt a different conformation in solution. The deviation from the theoretical neutral point at N:COOH = 1:1 towards B-PEI-rich mixtures had been previously described for other B-PEI-containing PIC nanoparticles,<sup>[29]</sup> and it is likely a result of the incomplete protonation of all amines in B-PEI due to Coulombic interactions between neighboring ammonium groups.<sup>[30]</sup> Similarly, since peptides with higher multivalencies should have stronger affinities for B-PEI, the exchange of the peptides with higher multivalency (i.e. P3<sub>SH</sub> and P4<sub>SH</sub>) between PIC nanoparticles and the solution should be slower than for the smaller peptides, thus trapping colloiddally stable intermediates even at N:COOH ratios that should favor the formation of neutral PIC nanoparticles. Additionally, P3<sub>SH</sub> and P4<sub>SH</sub> showed no significant difference in the size or charge of any of the resulting PIC nanoparticles (Figure 3), suggesting that multivalency is the predominant factor that governs the self-assembly of this collection of peptides. Regardless of the peptide used, no PIC nanoparticles could be detected at a 1:0.2 N:COOH ratio, probably as a result of the incomplete complexation of polyelectrolytes at this low concentration of peptide. The polydispersity indices (PDIs) of all PIC nanoparticles ranged between 0.01–0.06 with the exception of the formulations prepared at a 1:0.3 N:COOH ratio, which displayed significantly higher PDI values of up to 0.17 (Table S1). It was clear from dynamic light scattering (DLS) studies that formulations with

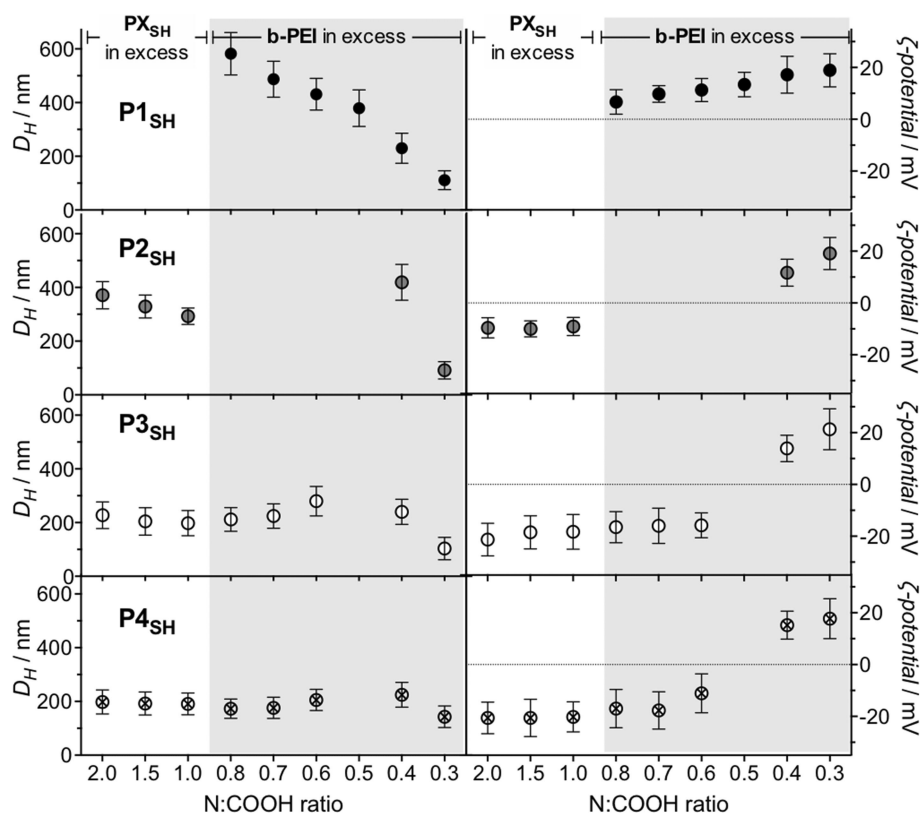


**Figure 3.** Hydrodynamic diameter ( $D_H$ , left) and  $\zeta$ -potential (right) of PIC nanoparticles prepared from peptides  $P1_{SH}$ – $P4_{SH}$  at different N:COOH ratios. Each value represents the mean size and charge of the only population fitted by the software for each sample  $\pm$  its standard deviation. Empty spaces indicate formulations that did not form PIC particles. Further details can be found in Table S1. Results obtained directly after the assembly of the nanoparticles without prior filtration. Data for  $P1_{SH}$  reproduced from I. Insua, E. Lamas, Z. Zhang, A. F. Peacock, A. M. Krachler, F. Fernandez-Trillo, *Polym Chem* **2016**, *7*, 2684–2690 – Published by The Royal Society of Chemistry.

lower peptide contents led to broader size distributions, although this phenomenon was less pronounced as the net charge of the peptide increased (Figure S6).

Size-wise,  $P2_{SH}$ – $P4_{SH}$  formulations showed a smaller variability in size than those reported for  $P1_{SH}$  (Figure 3). Particles with larger hydrodynamic diameters ( $D_H$ ) were obtained for  $P2_{SH}$  (ca. 300–400 nm) than for  $P3_{SH}$  and  $P4_{SH}$  (ca. 100–300 nm), regardless of the N:COOH ratio tested (Figure 3). Nanoparticles of smaller size for these two peptides could be the result of their higher multivalency (7 COOH groups for  $P3_{SH}$  and  $P4_{SH}$  versus 5 for  $P2_{SH}$  and 3 for  $P1_{SH}$ ), which would result in more strongly and tightly bound polyelectrolyte networks within these nanoparticles. For all peptides, formulations prepared at a 1:0.3 N:COOH ratio gave the smallest PIC nanoparticles, with an average  $D_H$  of ca. 110 nm and  $\zeta$ -potential of +19 mV – in agreement with the values previously found for  $P1_{SH}$  at this N:COOH ratio.<sup>[18]</sup>

### Structural Characterization of PIC Particles

To further understand the impact that the multivalency and cross-linking units of peptides  $P1_{SH}$ – $P4_{SH}$  have on the structure of the PIC nanoparticles formed, these materials were characterized by Static Light Scattering (SLS). Multi-angle SLS analysis

of nanomaterials allows the calculation of their radius of gyration ( $R_g$ ) by deconvolution of the Zimm equation (Eq. 1),<sup>[31,32]</sup> where  $K$  is a constant containing the optical parameters,  $c$  is the concentration of the sample,  $R_\theta$  the Rayleigh ratio of the particles at a given scattering angle ( $\theta$ ),  $q$  is the scattering wave vector and  $Mw_{PIC}$  is the average molecular weight of the nanoparticles. Thus, the ratio between gyration and hydrodynamic radii (i.e.  $R_g/R_H$ ), calculated by SLS and DLS respectively, provides valuable information about the internal structure and shape of nanomaterials.<sup>[31]</sup>

$$\frac{Kc}{R_\theta} = \frac{Rg^2}{3 Mw_{PIC}} \times q^2 + \frac{1}{Mw_{PIC}} \quad (1)$$

PIC nanoparticles prepared from all four peptides at a 1:0.3 N:COOH ratio were selected for SLS analysis, being the most consistent formulation throughout the collection of peptides studied. The scattering intensity from a suspension of PIC nanoparticles was measured at different angles ranging from 20 to 100°, and their DLS profiles were simultaneously recorded. Unfortunately, non-linear Zimm plots were obtained for all PIC particle samples with deviations at low angles, which made impossible the accurate measurement of  $Mw_{PIC}$  and  $R_g$  (Figure S7). Since larger particles have higher scattering contributions at low angles,<sup>[32]</sup> we considered that this non-linearity



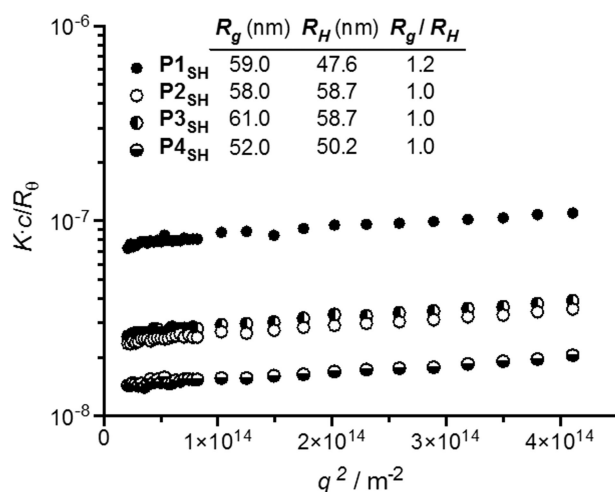


**Figure 4.** Partial Zimm plots obtained by SLS of filtered PIC particles prepared from peptides **P1<sub>SH</sub>**–**P4<sub>SH</sub>** at a 1:0.3 N:COOH ratio. The inset indicates the gyration ( $R_g$ ) and hydrodynamic ( $R_H$ ) radii simultaneously calculated by SLS and DLS, respectively.

could be corrected by filtering the samples through membranes with a pore size of 0.45  $\mu\text{m}$ , and thus remove any scatterers larger than the expected nanoparticles – which were all smaller than the filter's cut-off size according to our previous DLS characterization (Figure 3). All filtered samples of PIC nanoparticles displayed linear Zimm plots that allowed the calculation of their  $R_g$ , which was then compared with the  $R_H$  obtained by DLS under the same conditions (Figure 4). The average  $R_H$  measured from filtered samples was 57.5 nm, which is in agreement with the  $D_H$  previously obtained from unfiltered nanoparticles (*ca.* 110 nm), suggesting that the filtration did not affect the main composition of PIC nanoparticles in the samples.

Nanoparticles prepared from peptides **P2<sub>SH</sub>**–**P4<sub>SH</sub>** consistently showed an  $R_g/R_H$  value of 1.0, whereas those containing the peptide **P1<sub>SH</sub>** presented a slight deviation towards  $R_g/R_H > 1$ , which is characteristic of anisotropic nanomaterials.<sup>[31]</sup> This difference can be explained from the tendency of the latter nanoparticles to aggregate, as observed when their  $D_H$  was monitored over time (Figure S8): Whereas PIC nanoparticles prepared from peptides **P2<sub>SH</sub>**–**P4<sub>SH</sub>** displayed the same size over time, the  $D_H$  of the nanoparticles made from **P1<sub>SH</sub>** increased by 50% after 10 days, which was the time that passed between the preparation of these PIC nanoparticles and their SLS analysis. Nevertheless, the  $R_g/R_H$  values found for this collection of nanoparticles are in agreement with those reported in the literature for other PIC nanoparticles (1.0–1.6).<sup>[33,34]</sup> These  $R_g/R_H$  ratios, which are higher than the value expected for a solid sphere (0.775),<sup>[31]</sup> have been rationalized by the high polydispersity of PIC nanoparticles and their tendency to aggregate in some cases.<sup>[33,35]</sup> Both of these factors act as a bias towards higher  $R_g/R_H$  values, making the elucidation of the internal structure of these nanomaterials extremely difficult.

In summary, the structural characterization of these nanoparticles by SLS and DLS indicates that all formulations have very similar  $R_g$  and  $R_H$  regardless of the peptide used, and

therefore no distinct structural features should be expected in any of these complexes.

### Stability under Physiological Conditions of PIC Particles

The electrostatic forces that keep PIC nanoparticles together can be shielded by small electrolytes, leading to swelling and ultimately breakdown of these nanoparticles.<sup>[36]</sup> Hence, the integrity of PIC nanoparticles is often compromised by the concentrations of salts present in biological fluids. This lack of stability was the case for our previously reported nanoparticles, for which only one of the formulations was stable under simulated physiological conditions (Figure 5 and Figure S9, **P1<sub>SH</sub>**, 0.3 N:COOH ratio). The tolerance to physiological conditions of the new nanoparticles was evaluated by incubation in the presence of 154 mM NaCl at 37 °C, and the change of  $D_H$  was monitored over four hours (Figure 5).

All PIC nanoparticles swelled when exposed to NaCl and this swelling was inversely proportional to the peptides' multivalency and the degree of cross-linking in the particle. As predicted, increasing the multivalency in the peptide resulted in tighter nanoparticles, that swelled less in the presence of NaCl (Figure 5). For all peptides, nanoparticles made at a 1:0.3 N:COOH ratio swelled the most, with particles prepared from **P2<sub>SH</sub>** and **P3<sub>SH</sub>** becoming over 20 times bigger after 4 hours of incubation (Figure 5A), a similar increase in size to that reported for **P1<sub>SH</sub>**. Interestingly, those prepared from **P4<sub>SH</sub>**, which carries an extra cysteine and should give higher cross-linking densities at the same N:COOH ratio, were the least affected by this saline medium, regardless of the formulation employed (Figure 5, ⊗).

Overall, all the particles prepared with the new peptides **P2<sub>SH</sub>**–**P4<sub>SH</sub>** showed better physiological stabilities than those previously reported for trivalent **P1<sub>SH</sub>** (Figure 5, ●),<sup>[18]</sup> reinforcing the correlation between peptide multivalency and PIC nanoparticle stability (Figure 5 and Figure S9). Particles prepared from the least multivalent peptide **P2<sub>SH</sub>** showed more polydisperse aggregates after 2 and 3 hours and, for those prepared at a 1:1 N:COOH ratio, no particles could be detected after 4 hours of incubation under these conditions (Figure 5E, ●). These results highlight the critical effect that multivalency and cross-linking degree have on the salt tolerance of PIC particles, as evidenced by their physiological stability: **P1<sub>SH</sub>** < **P2<sub>SH</sub>** < **P3<sub>SH</sub>** < **P4<sub>SH</sub>**.

### Stability Upon Freeze-drying

Finally, we evaluated if the increase in stability observed under physiological conditions for the nanoparticles formed with the new peptides **P2<sub>SH</sub>**–**P4<sub>SH</sub>** could be correlated to an increased stability upon storage. Nanoparticles prepared at a 1:0.3 N:COOH ratio were selected for this evaluation, being a consistent formulation across all peptides evaluated. Also, nanoparticles prepared at this N:COOH ratio have the least amount of peptide and while stable, swelled more upon incubation in physiological conditions. This swelling may

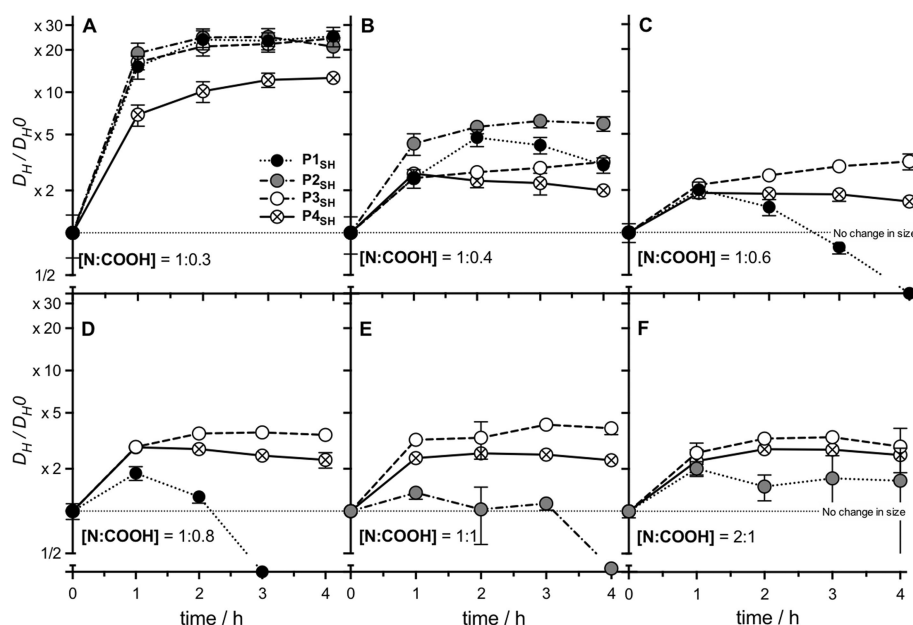


**Figure 5.** Relative change in size ( $D_H/D_{H0}$ ) for PIC particles prepared from peptides  $P1_{SH}$ – $P4_{SH}$  at representative N:COOH ratios under simulated physiological conditions (37 °C, 154 mM NaCl, pH 7.4) (A 1:0.3 [N:COOH] ratio, B 1:0.4 [N:COOH] ratio, C 1:0.6 [N:COOH] ratio, D 1:0.8 [N:COOH] ratio, E 1:1 [N:COOH] ratio and F 2:1 [N:COOH] ratio). Particle size ( $D_H$ ) was normalized to that of the PIC particles in the absence of NaCl (0 hours, No change in size).  $n=3$ , mean values  $\pm$  standard deviation. Results obtained directly after the assembly of the nanoparticles without prior filtration. Data for  $P1_{SH}$  reproduced from I. Insua, E. Lamas, Z. Zhang, A. F. Peacock, A. M. Krachler, F. Fernandez-Trillo, *Polym Chem* **2016**, 7, 2684–2690 – Published by The Royal Society of Chemistry.

indicate that the cohesive forces in the core of these nanoparticles are weak enough to accommodate the presence of competing counterions, or a higher tendency to aggregate, making it an ideal formulation to test stability. To this end, freshly prepared nanoparticles at this N:COOH ratio were allowed to stand in a dark, cool and dry place, and their size monitored over time (Figure S8). As described before, no change in size was observed for any the nanoparticles prepared with the new peptides  $P2_{SH}$ – $P4_{SH}$ , even after 10 days of storage. This was not the case for the nanoparticles prepared with  $P1_{SH}$  which quickly increased in size.

Nanoparticles prepared from  $P3_{SH}$  at a 0.3 N:COOH ratio, which showed excellent stability in solution, were then selected as a representative example to evaluate the potential of these formulations to be stored as a powder. Therefore, freshly prepared nanoparticles from  $P3_{SH}$  at a 0.3 N:COOH ratio were freeze-dried overnight to yield a white powder. Approximately 1.32 mg of powder were recovered for all 3 samples prepared (standard deviation 0.042), in close agreement with the 1.47 mg expected taking into account the amount of peptide and B-PEI used, and how much solid content was in the buffer used to prepare the nanoparticle suspension. This powder was then reconstituted in deionized water to give the original volume (1 mL). Samples were then gently resuspended on a roller for 30 mins and characterized via DLS and  $\zeta$ -potential. A small increase in size was observed following resuspension (Figure 6A, ●) in agreement with the small shift in the autocorrelation curve (Figure 6D), while no changes in the  $\zeta$ -potential of the particles were observed following resuspension on the rollers (Figure 6B, ●). A bigger effect was observed on the number of counts, which decreased from  $402.8 \pm 2.3$  to  $54.2 \pm$

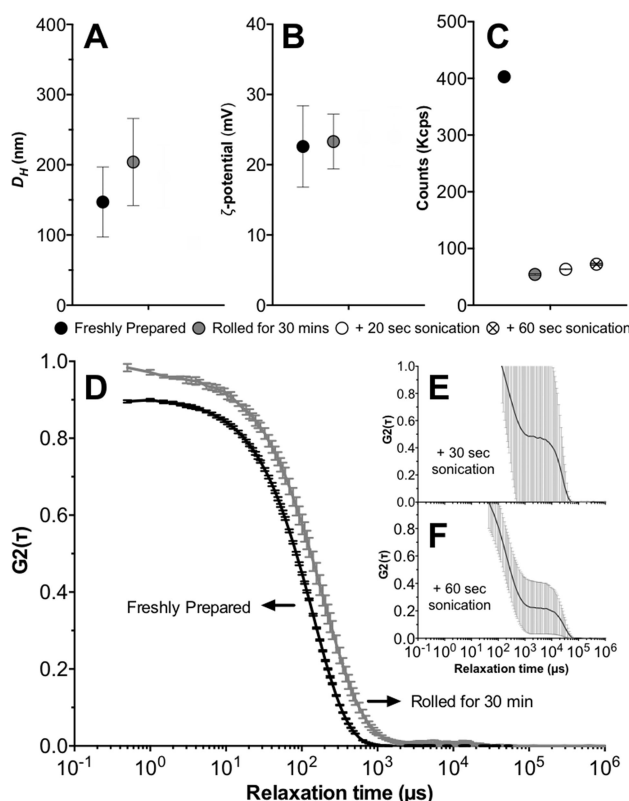


**Figure 6.** Effect of freeze-drying and resuspension of the size (A),  $\zeta$ -potential (B) and number of counts (C) of nanoparticles prepared with  $P3_{SH}$  at a 0.3 N:COOH ratio. Autocorrelation function curves for freshly prepared and nanoparticles following resuspension on a roller for 30 mins (D) and additional sonication for 30 sec (E) or 60 secs (F).

1.2 (Figure 6C, ●) suggesting that less particles were available in suspension following reconstitution.

These samples were then sonicated for 30 or 60 seconds to try to increase the number of nanoparticles in suspension. While a small increase in the number of counts was observed (Figure 6C, ○ and ⊗ for 30 and 60 secs respectively), sonication had a detrimental effect on the nanoparticles and very noisy autocorrelation function curves were obtained (Figure 6E and F), which prevented accurate characterization of their size and  $\zeta$ -potential (Figure 6A and B).

## Conclusions

Three new enzyme-responsive anionic peptides (**P2<sub>SH</sub>**–**P4<sub>SH</sub>**) have been synthesized and their use in the preparation of PIC nanoparticles containing the antimicrobial polymer B-PEI reported. These peptides were designed to incorporate the LasB-degradable sequence –GLA–, and increasing amounts of glutamic acids for a stronger interaction with B-PEI (**P2<sub>SH</sub>** and **P3<sub>SH</sub>**), and an additional cysteine (**P4<sub>SH</sub>**) to generate PIC nanoparticles with higher cross-linking density. The enzymatic degradation of these peptides was assessed against bacterial (LasB) and human (HLE) elastases and, while all peptides were degraded by the bacterial elastase, no direct correlation with the multivalency of the peptides could be identified. All new peptides formed PIC nanoparticles when incubated with B-PEI, and a broad range of formulations could be accessed by varying the ratio of polyelectrolytes (i.e. N:COOH ratio). Our results show that these new peptides allow the preparation of negatively charged nanoparticles, not previously accessible using the less multivalent peptide **P1<sub>SH</sub>**, previously reported by our group.<sup>[18]</sup> More importantly, the stability of the new nanoparticles under simulated physiological conditions increased with increasing multivalency and cross-linking degree of the peptides (i.e. **P2<sub>SH</sub>** < **P3<sub>SH</sub>** < **P4<sub>SH</sub>**) and displayed higher saline stability than those prepared using **P1<sub>SH</sub>**. The structural analysis of these peptides and their resulting PIC nanoparticles by CD and SLS, respectively, suggests that there are no differences in conformation or architecture across the whole collection of materials tested that could explain these differences in susceptibility against LasB and stability. Finally, the stability of representative formulations upon storage was evaluated. Our results demonstrate the importance of carefully optimizing peptide sequence and multivalency in the design of peptide-based PIC particles and we believe these new peptides and formulations will underpin the future development of “smart” delivery systems for antimicrobials. Our efforts to identify LasB-responsive nanoparticles with optimized release and antimicrobial activity, as well as the application of these peptides for the preparation of other delivery systems, will be reported in due course.

## Experimental Section

### Materials

Enzymes (*Pseudomonas aeruginosa* Elastase (LasB): EC 3.4.24.26 and Human Leucocyte Elastase (HLE): EC 3.4.21.37) were purchased from Merck Millipore. Branched poly(ethylene imine) 25 kDa average molecular weight (B-PEI) and 4-(2-hydroxyethyl)piperazine-1-ethanesulfonic acid (HEPES) were bought from Sigma-Aldrich®. Fluorescamine and dimethylsulphoxide (DMSO) were purchased from Acros Organics™. Ethylenediaminetetraacetic acid (EDTA) was purchased from Alfa Aesar®. Nylon 0.45  $\mu$ m syringe filters were purchased from Camlab.

### Instrumentation

Dynamic Light Scattering (DLS) and  $\zeta$ -potential measurements were carried out with a Zetasizer Nano ZSP (Malvern Instruments Ltd.) stabilized at 37 °C. DLS was read at 173° (backscattering) for 60 seconds in triplicate and  $\zeta$ -potentials were averaged from 30 measurements at 140 V. DLS correlograms were processed with Malvern's *General Purpose* non-negative least squares algorithm, and their  $D_h$  values correspond to the mean size and standard deviation of the only population found in their size-intensity plots. A FLUOstar Omega (BMGLabtech GmbH) microplate reader was used to incubate and measure fluorescamine reactions. Static Light Scattering (SLS) and simultaneous DLS data was collected using an CGS-3 Compact Goniometer System (ALV GmbH) stabilized at 20 °C and operating at a wavelength of 633 nm against a toluene standard.

### Preparation of PIC Nanoparticles

For nanoparticles prepared at a 1:0.3 N:COOH ratio (defined as the ratio between amines in B-PEI and carboxylic acids in the peptides), stock solutions of B-PEI (2.5 mM in amines) and peptide (**P1<sub>SH</sub>**–**P4<sub>SH</sub>**) (0.75 mM in carboxylate groups) in 5 mM HEPES buffer at pH 7.4 were prepared. Then, both solutions were filtered and mixed in equal volumes drop-wise under stirring. The reaction mixture was stirred at room temperature for 24 hours open to air to allow thiol oxidation. PIC nanoparticles prepared at different N:COOH ratios were obtained by changing the concentration of peptide stock solution and mixing with the 2.5 mM B-PEI stock following the same protocol (Table S1). After 24 hours, samples were analyzed directly by DLS and  $\zeta$ -potential without prior filtration.

### Enzymatic Degradation of Peptides – Fluorescamine Assay

Stock solutions of peptide (1 mM) or succinyl casein (0.5 mg/mL) were prepared in 25 mM Na<sub>2</sub>B<sub>4</sub>O<sub>7</sub> buffer at pH 8.0 with 10 mM CaCl<sub>2</sub> and 10% v/v DMSO. 125  $\mu$ L of these substrate solutions were added to a 96-well black-walled microplate and mixed with 125  $\mu$ L of the same buffer without DMSO, containing 15  $\mu$ g of enzyme (LasB or HLE). Solutions of enzymes and substrates alone were prepared as controls. Every sample was prepared in triplicate. The microplate was incubated at 37 °C for 4 hours under orbital shaking. After 4 hours, 50  $\mu$ L of 0.1 M EDTA in water at pH 8.0 were added to each well to quench all enzymatic activity. Then, each sample was mixed in a 1:1 volume ratio with a 1 mM solution of fluorescamine<sup>[19]</sup> in methanol. The microplate was incubated at 37 °C under orbital shaking for 30 minutes. After this time, fluorescence was measured exciting at 355 nm and reading the emission at 460  $\pm$  10 nm.



## Stability of PIC Nanoparticles in Simulated Physiological Conditions

182  $\mu\text{L}$  of a 1 M solution of NaCl in water was added to a sample of PIC nanoparticles (1 mL), prepared as described above. This mixture was then incubated at 37 °C to obtain physiological osmotic pressure and temperature. Every hour, the sample was analyzed by DLS as described above.

## Freeze-drying and Resuspension of PIC Nanoparticles

A sample (1 mL) of freshly made PIC nanoparticles from P3<sub>SH</sub> and B-PEI at a 1:0.3 N:COOH ratio was frozen inside a tared 2 mL-scintillation vial, to be then left overnight under vacuum at –80 °C. A white solid was thus obtained, which was weighed by difference inside the tared vial. Then, 1 mL of deionized water was added to the vial and the mixture was gently and simultaneously rocked and rolled for 30 min. After this time, the sample was characterized by DLS and  $\zeta$ -potential as indicated above. Replicates of this freeze-dried and reconstituted sample were further processed by immersion in an ultrasonic bath at room temperature for 30 and 60 sec, and characterized likewise. For the measurement of light scattering intensity by DLS (i.e. counts, Figure 6C), the attenuator value of the instrument was kept constant across all measurements.

## Author Contributions

All authors contributed to the experimental set-up and discussed the results. II and MP synthesized and characterized the peptides. II and FFT designed the peptides, and the nanoparticle preparation and characterization. II, FFT and AMK designed the enzymatic assays. LDB, RK, APB and RKOR designed and performed structural characterization. II carried out all other experiments. FFT and AMK secured funding. II and FFT analyzed the data and wrote the paper, with all other authors contributing to the final version of the manuscript.

## Acknowledgements

This work was supported by the Wellcome Trust (177ISSFPP), the Engineering and Physical Sciences Research Council (EPSRC) (EP/N508755/1), the Birmingham Science City and the European Regional Development Fund, and the University of Birmingham (FFT and II, John Evans Fellowship; AMK, Birmingham Fellowship). The authors thank Dr Marie-Christine Jones and Dr Hanene Ali-Boucetta (School of Pharmacy, UoB) for the access to the DLS, and Nicolas Perez-Soto for useful discussions.

## Conflict of Interest

The authors declare no conflict of interest.

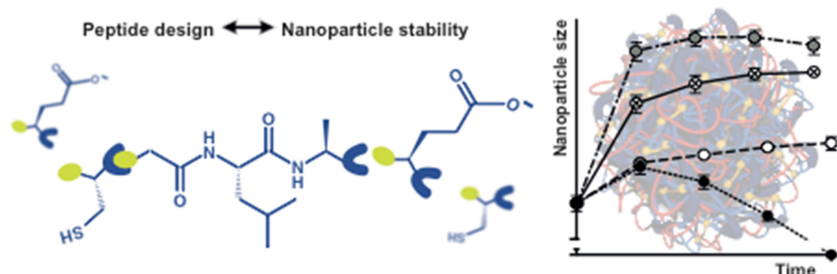
**Keywords:** Nanoparticles • Enzymes • Polyelectrolytes • Self-assembly • Drug delivery

## References

- [1] A. D. Kulkarni, Y. H. Vanjari, K. H. Sancheti, H. M. Patel, V. S. Belgamwar, S. J. Surana, C. V. Pardeshi, *Artif. Cells, Nanomed., Biotechnol.* **2016**, *44*, 1615–1625.
- [2] D. V. Pergushov, A. H. E. Müller, F. H. Schacher, *Chem. Soc. Rev.* **2012**, *41*, 6888–6901.
- [3] I. Insua, A. Wilkinson, F. Fernández-Trillo, *Eur. Polym. J.* **2016**, *81*, 198–215.
- [4] S. C. How, Y. F. Chen, P. L. Hsieh, S. S. S. Wang, J.-S. Jan, *Colloids Surf. B* **2017**, *153*, 244–252.
- [5] L. Zhang, J. Wang, C. Ni, Y. Zhang, G. Shi, *Mater. Sci. Eng. C* **2016**, *58*, 724–729.
- [6] L. Yang, S. Gao, S. Asghar, G. Liu, J. Song, X. Wang, Q. Ping, C. Zhang, Y. Xiao, *Int. J. Biol. Macromol.* **2015**, *72*, 1391–1401.
- [7] Y.-H. Hsieh, Y.-T. Hsiao, J.-S. Jan, *Soft Matter* **2014**, *10*, 9568–9576.
- [8] I. Insua, S. Majok, A. F. A. Peacock, A. M. Krachler, F. Fernández-Trillo, *Eur. Polym. J.* **2017**, *87*, 478–486.
- [9] K. A. Les, A. H. A. Mohamed-Ahmed, S. Balan, J.-W. Choi, D. Martin, V. Yardley, K. Powell, A. Godwin, S. J. Brocchini, S. Brocchini, *Polym. Chem.* **2014**, *5*, 1037–1048.
- [10] K. L. Niece, A. D. Vaughan, D. I. Devore, *J. Biomed. Mater. Res. A* **2013**, *101*, 2548–2558.
- [11] I. Insua, L. Zismare, A. F. A. Peacock, A. M. Krachler, F. Fernández-Trillo, *Sci. Rep.* **2017**, *7*, 9396–10.
- [12] A. Carmona-Ribeiro, J. Sampaio, H. Santos, L. Carrasco, *Drug Delivery Letters* **2017**, *7*, 39–47.
- [13] E. F. Craparo, B. Porsio, D. Schillaci, M. G. Cusimano, D. Spigolon, G. Giammona, G. Cavallaro, *Nanomedicine* **2017**, *12*, 25–42.
- [14] D. Vehlou, R. Schmidt, A. Gebert, M. Siebert, K. S. Lips, M. Müller, *Nanomaterials* **2016**, *6*, 53.
- [15] U. Lächelt, E. Wagner, *Chem. Rev.* **2015**, *115*, 11043–11078.
- [16] R. V. Ulijn, *J. Mater. Chem.* **2006**, *16*, 2217–2225.
- [17] W. E. Kaman, J. P. Hays, H. P. Endtz, F. J. Bikker, *Eur. J. Clin. Microbiol. Infect. Dis.* **2014**, *33*, 1081–1087.
- [18] I. Insua, E. Lamas, Z. Zhang, A. F. A. Peacock, A. M. Krachler, F. Fernández-Trillo, *Polym. Chem.* **2016**, *7*, 2684–2690.
- [19] S. Udenfriend, S. Stein, P. Böhlen, W. Dairman, W. Leimgruber, M. Weigle, *Science* **1972**, *178*, 871–872.
- [20] K. Morihara, H. Tsuzuki, *Arch. Biochem. Biophys.* **1971**, *146*, 291–296.
- [21] S. Suter, U. B. Schaad, L. Roux, U. E. Nydegger, F. A. Waldvogel, *J. Infect. Dis.* **1984**, *149*, 523–531.
- [22] N. J. Greenfield, *Nat. Protoc.* **2006**, *1*, 2876–2890.
- [23] B. Korkmaz, S. Attucci, T. Moreau, E. Godat, L. Juliano, F. Gauthier, *Am. J. Respir. Cell Mol. Biol.* **2004**, *30*, 801–807.
- [24] B. Korkmaz, S. Attucci, E. Hazouard, M. Ferrandière, M. L. Jourdan, M. Brillard-Bourdet, L. Juliano, F. Gauthier, *J. Biol. Chem.* **2002**, *277*, 39074–39081.
- [25] K. Morihara, H. Tsuzuki, T. Oka, H. Inoue, M. Ebata, *J. Biol. Chem.* **1965**, *240*, 3295–3304.
- [26] B. Wretling, T. Wadström, *J. Gen. Microbiol.* **1977**, *103*, 319–327.
- [27] E. Kessler, D. E. Ohman, in *Handbook of Proteolytic Enzymes*, Elsevier, **2013**, pp. 582–592.
- [28] M. Müller, *Polyelectrolyte Complexes in the Dispersed and Solid State II*, Springer, Berlin, **2013**.
- [29] H. Sato, A. Nakajima, *Polym. J.* **1975**, *7*, 241–247.
- [30] M. Borkovec, G. Koper, *Macromolecules* **1997**, *30*, 2151–2158.
- [31] J. P. Patterson, M. P. Robin, C. Chassenieux, O. Colombani, R. K. O'Reilly, *Chem. Soc. Rev.* **2014**, *43*, 2412–2425.
- [32] B. H. Zimm, *J. Chem. Phys.* **1948**, *16*, 1099–1116.
- [33] K. Ueno, H. Ueno, T. Sato, *Polym. J.* **2012**, *44*, 59–64.
- [34] D. Fischer, H. Dautzenberg, K. Kunath, T. Kissel, *Int. J. Pharm.* **2004**, *280*, 253–269.
- [35] H. Dautzenberg, J. Kriz, *Langmuir* **2003**, *19*, 5204–5211.
- [36] H. Dautzenberg, G. Rother, *Macromol. Chem. Phys.* **2004**, *205*, 114–121.

Manuscript received: February 4, 2018  
Version of record online: April 23, 2018

## FULL PAPER



**PIC-a-boo!** A series of anionic peptides degradable by a bacterial protease were incubated with a cationic polymer, and the effect of peptide multivalency on the structure and stability of the resulting self-assembled polyion complex (PIC) nanoparticles was investigated.

Changes in the charge (i.e., number of glutamic acids) and cross-linking (i.e., cysteine content) of the peptides gave access to PIC nanoparticles with remarkably improved saline stability and good tolerance to dry storage without any apparent effect on their internal structure.

### Peptide Nanoparticles

Dr. I. Insua, M. Petit, Dr. L. D. Blackman, R. Keogh, Dr. A. Pitto-Barry, Prof. R. K. O'Reilly, Dr. A. F. A. Peacock, Dr. A. M. Krachler, Dr. F. Fernandez-Trillo\*

1 – 9

**Structural Determinants of the Stability of Enzyme-Responsive Polyion Complex Nanoparticles Targeting *Pseudomonas aeruginosa*'s Elastase**



# **Structural determinants of the stability of enzyme-responsive polyion complex (PIC) nanoparticles targeting *Pseudomonas aeruginosa*'s elastase**

Ignacio Insua,<sup>[a],[b]</sup> Marion Petit,<sup>[a]</sup> Lewis D. Blackman,<sup>[c]</sup> Robert Keogh,<sup>[c]</sup> Anaïs Pitto-Barry,<sup>[c]</sup> Rachel K. O'Reilly,<sup>[c]</sup> Anna F. A. Peacock,<sup>[a]</sup> Anne Marie Krachler,<sup>[b],[d]</sup> and Francisco Fernandez-Trillo<sup>\*[a],[b]</sup>

*[a] School of Chemistry, University of Birmingham, Edgbaston, B15 2TT, UK. [b] Institute of Microbiology and Infection – School of Biosciences, University of Birmingham, Edgbaston, B15 2TT, UK. [c] School of Chemistry, University of Warwick, Coventry, CV4 7AL, UK. [d] Current address: Department of Microbiology and Molecular Genetics, University of Texas Health Science Center, 6431 Fannin. Houston (TX), USA*

*\*Email: f.fernandez-trillo@bham.ac.uk*

1. Materials .....	2
2. Instrumentation .....	2
3. Peptide synthesis.....	2
4. Peptide characterisation.....	2
5. Enzymatic degradation of peptides .....	6
6. Circular dichroism characterisation of peptides.....	7
7. PIC particle characterisation .....	8
8. SLS characterisation of unfiltered PIC particles .....	9
9. Shelf stability of PIC particles .....	10
10. Stability of the particles under physiological conditions.....	10
11. Additional references.....	11

## 1. Materials

*N*-Fmoc-protected L-amino acids were purchased from Merck Millipore. *N,N*-dimethylformamide (DMF), piperidine 20% v/v in DMF and acetic anhydride were purchased from Sigma-Aldrich®. H-L-Cys(Trt)-2-chlorotrityl resin (0.49 mmol/g) was bought from AGTC Bio Products Ltd. *N,N*-diisopropylethylamine (DIPEA), triisopropylsilane (TIPS), 1,2-ethanedithiol (EDT) and trifluoroacetic acid (TFA) were bought from Alfa Aesar®. *N,N,N',N'*-tetramethyl-*O*-(1*H*-benzotriazol-1-yl)uronium hexafluorophosphate (HBTU) was purchased from Carbosynth Ltd. All other chemicals were purchased from Fisher Scientific UK Ltd. and were used without further purification.

## 2. Instrumentation

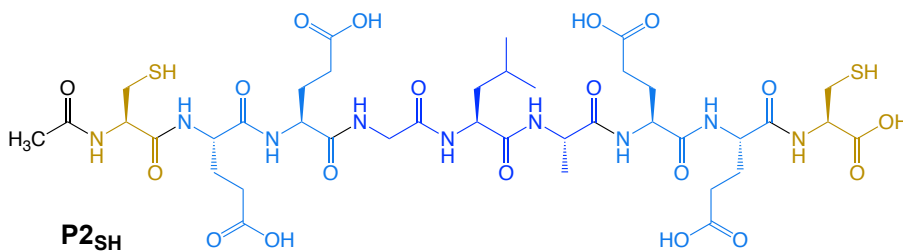
NMR data was acquired on a Bruker Avance III operating at 400 MHz and fitted with a 5 mm DUL probe (<sup>1</sup>H/<sup>13</sup>C). MS spectra were obtained on a Xevo® G2-XS ToF (Waters) from electrospray ionisation (ESI) and time-of-flight (TOF) measurement in positive ion mode. High-resolution MS data was calculated by comparison with leucine-enkephalin as internal standard. Reverse phase (RP) HPLC analysis was run through a Kinetex® C18-EVO column (Phenomenex®): 5 µm, 100 Å, 250x4.60 mm. A gradient from 3 to 20% of (CH<sub>3</sub>CN + 0.05% TFA) in (H<sub>2</sub>O + 0.05% TFA) was used at 1 mL/min. The column was maintained at 35°C and UV-VIS detection was set at 210 nm. Circular dichroism spectra were recorded in 1 mm path length quartz cuvettes on a Jasco J-715 spectropolarimeter. The observed ellipticity in millidegrees was converted into mean residue ellipticity and it is reported in units of degree · dmol<sup>-1</sup> · cm<sup>2</sup> · residue<sup>-1</sup>.<sup>[1]</sup>

## 3. Peptide synthesis

500 mg of H-L-Cys(Trt)-2-chlorotrityl resin (0.245 mmol) were swollen in 5 mL of DMF for 30 minutes. Then, solutions of Fmoc-L-amino acid (3 eq), HBTU (2.8 eq) and DIPEA (2.8 eq) in DMF were added to a final volume of 5 mL. The reaction mixture was rolled for 1 h at room temperature, after which a negative chloranil test<sup>[2]</sup> indicated the reaction had gone to completion. The *N*-terminal Fmoc protecting group was removed by washing the resin with 5 mL of piperidine 20% v/v in DMF during 10 minutes. A positive chloranil test confirmed the removal of the Fmoc group, and the previous steps were repeated to couple all amino acids in the sequence. Following the coupling of the last amino acid, the Fmoc group was removed and the terminal amine of the peptide was capped by reacting with 5 mL of acetic anhydride:DIPEA:DMF (1:1:3) for 1 h at room temperature. Then, the resin was thoroughly washed with DMF and diethyl ether, and the peptide was cleaved from the resin with 5 mL of a mixture containing TFA (80%), TIPS (8%) and EDT (12%) for 2 h. After this time, the solution was concentrated under argon and precipitated in chilled diethyl ether:hexane (1:4). Finally, the suspension was centrifuged and the pellets were washed twice with diethyl ether:hexane (1:4), dissolved in water and freeze-dried. Peptides that showed impurities by <sup>1</sup>H-NMR (e.g. trityl protecting groups) were further purified by dissolving the material in 2 mL of a 10% TIPS solution in TFA and precipitating in chilled diethyl ether:hexane (1:4), to be then centrifuged and freeze-dried as explained above. Peptide purity was determined by HPLC.

## 4. Peptide characterisation

The synthesis and characterisation of peptides **P1<sub>SH</sub>** (Ac-CEGLAEC-OH) and **P5** (H<sub>2</sub>N-LAE-OH) has been previously reported.<sup>[3]</sup>



**P2<sub>SH</sub>, Ac-CEEGLAEEC-OH** (154.8 mg, 62% yield) **<sup>1</sup>H-NMR** (400 MHz, DMSO-*d*<sub>6</sub>): δ 0.84(dd, *J*=15.0, 6.5 Hz, 6H, H<sup>δ</sup>-Leu); 1.20(d, *J*=7.1 Hz, 3H, H<sup>β</sup>-Ala 1.35-1.47(m, 2H, H<sup>β</sup>-Leu); 1.50-1.63(m, 1H, H<sup>γ</sup>-Leu); 1.66-1.80(m, 4H, H<sup>β</sup>-Glu); 1.84-1.96(m, 4H, H<sup>β</sup>-Glu); 1.87(s, 3H, Ac); 2.16-2.31(m, 8H, H<sup>γ</sup>-Glu); 2.36(t, *J*=8.5 Hz, 1H, SH); 2.45(t, *J*=8.6 Hz, 1H, SH); 2.62-2.89(m, 4H, H<sup>β</sup>-Cys); 3.70(ddd, *J*=56.8, 16.7, 5.7 Hz, 2H, H $\alpha$ -Gly); 4.20-4.41(m, 8H, H $\alpha$ ); 7.89(d, *J*=8.1 Hz, 1H, NHCO); 7.92(d, *J*=8.5 Hz, 1H, NHCO); 7.95(d, *J*=7.7 Hz, 1H, NHCO); 7.98(d, *J*=7.7 Hz, 1H, NHCO); 8.11-8.22(m, 5H, NHCO); 12.20(br.s, 4H, COOH) ppm. **<sup>13</sup>C-NMR** (400 MHz, DMSO-*d*<sub>6</sub>): δ 17.4(C $\beta$ -Ala); 21.4(H $\delta$ -Leu); 22.3(Ac); 22.9(H $\delta$ -Leu); 23.9(H $\gamma$ -Leu); 25.2(C $\beta$ -Cys); 25.9(C $\beta$ -Cys); 26.7(C $\beta$ -Cys); 27.2(C $\beta$ -Glu); 29.7(C $\gamma$ -Glu); 29.8(C $\gamma$ -Glu); 29.8(C $\gamma$ -Glu); 29.9(C $\gamma$ -Glu); 40.7(C $\beta$ -Leu); 41.6(C $\alpha$ -Gly); 48.0(C $\alpha$ ); 50.6(C $\alpha$ ); 51.4(C $\alpha$ ); 51.5(C $\alpha$ ); 51.8(C $\alpha$ ); 52.0(C $\alpha$ ); 54.2(C $\alpha$ ); 55.0(C $\alpha$ ); 168.5(NHCO); 169.8(Ac); 170.2(NHCO); 170.9(NHCO); 171.0(NHCO); 171.1(NHCO); 171.3(NHCO); 171.4(NHCO); 171.9(NHCO); 172.2(NHCO); 174.0(COOH) ppm. **MS** (ESI-TOF, +eV): *m/z* 1024.4 [M+H]<sup>+</sup>; 531.7 [M+Ca]<sup>2+</sup>. **HR-MS** (ESI-TOF, +eV): *m/z* 1024.3603 (calculated for [M+H]<sup>+</sup>); 1024.3605 (found). Purity by **HPLC** = 92% (R<sub>t</sub> = 24.2 min).

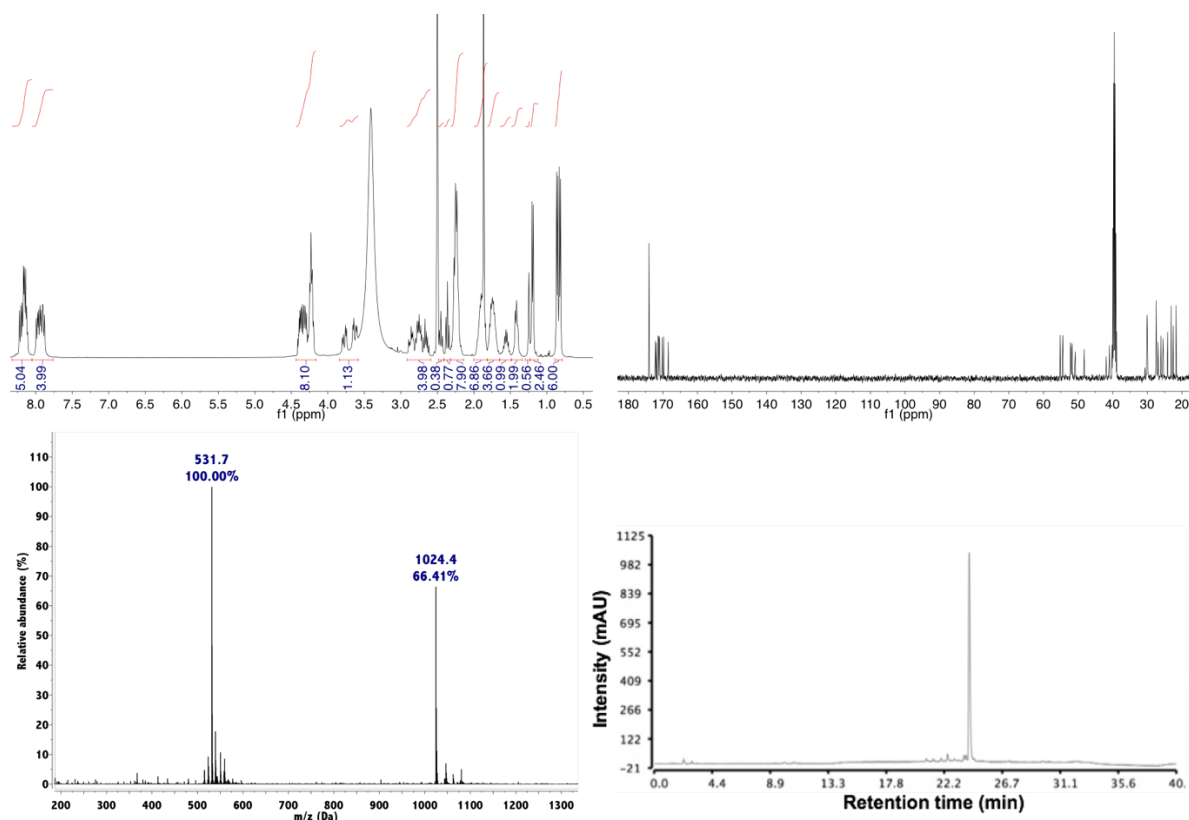
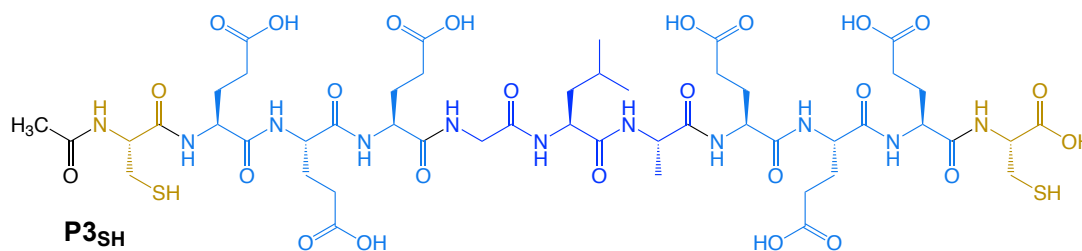


**Figure S1** Characterisation of peptide **P2<sub>SH</sub>** (Ac-C-EE-GLA-EE-C-OH). Top: <sup>1</sup>H (left) and <sup>13</sup>C (right) NMR spectra (400 MHz, DMSO-*d*<sub>6</sub>). Bottom: Mass spectrum (left) and RP-HPLC chromatogram (right).





**P3<sub>SH</sub>, Ac-CEEEGLAEEEC-OH** (152.5 mg, 72% yield) **<sup>1</sup>H-NMR** (400 MHz, DMSO-*d*<sub>6</sub>): δ 0.84(dd, *J*=14.8, 6.4 Hz, 6H, H<sup>δ</sup>-Leu); 1.19(d, *J*=7.0 Hz, 3H, H<sup>β</sup>-Ala); 1.36-1.47(m, 2H, H<sup>β</sup>-Leu); 1.50-1.63(m, 1H, H<sup>γ</sup>-Leu); 1.67-1.81(m, 6H, H<sup>β</sup>-Glu); 1.84-1.95(m, 6H, H<sup>β</sup>-Glu); 1.87(s, 3H, Ac); 2.17-2.29(m, 12H, H<sup>γ</sup>-Glu); 2.34(t, *J*=8.5 Hz, 1H, SH); 2.44(t, *J*=8.6 Hz, 1H, SH); 2.62-2.89(m, 4H, H<sup>β</sup>-Cys); 3.70(ddd, *J*=75.2, 16.7, 5.7 Hz, 2H, H<sup>α</sup>-Gly); 4.19-4.42(m, 10H, H<sup>α</sup>); 7.89-7.94(m, 4H, NHCO); 8.04(d, *J*=7.4 Hz, 1H, NHCO); 8.08(d, *J*=7.6 Hz, 1H, NHCO); 8.11-8.20(m, 5H, NHCO); 12.17(br.s, 5H, COOH) ppm. **<sup>13</sup>C-NMR** (400 MHz, DMSO-*d*<sub>6</sub>): δ 17.4(C<sup>β</sup>-Ala); 21.4(H<sup>δ</sup>-Leu); 22.3(Ac); 22.8(H<sup>δ</sup>-Leu); 23.9(H<sup>γ</sup>-Leu); 25.2(C<sup>β</sup>-Cys); 25.9(C<sup>β</sup>-Cys); 26.7(C<sup>β</sup>-Cys); 27.0(C<sup>β</sup>-Glu); 27.1(C<sup>β</sup>-Glu); 27.2(C<sup>β</sup>-Glu); 29.9 (C<sup>γ</sup>-Glu); 40.8(C<sup>β</sup>-Leu); 41.6(C<sup>α</sup>-Gly); 48.0(C<sup>α</sup>); 50.6(C<sup>α</sup>); 51.5(C<sup>α</sup>); 51.6(C<sup>α</sup>); 51.7(C<sup>α</sup>); 51.8(C<sup>α</sup>); 51.9(C<sup>α</sup>); 54.2(C<sup>α</sup>); 54.9(C<sup>α</sup>); 168.5(NHCO); 169.7(Ac); 170.1(NHCO); 171.0(NHCO); 171.0(NHCO); 171.2(NHCO); 171.4(NHCO); 171.4(NHCO); 171.9(NHCO); 172.3(NHCO); 174.0(COOH) ppm. **MS** (ESI-TOF, +eV): *m/z* 1282.4 [M+H]<sup>+</sup>; 668.7 [M+H+Na+CH<sub>3</sub>OH]<sup>2+</sup>; 660.7 [M+Ca]<sup>2+</sup>; 641.7 [M+2H]<sup>2+</sup>. **HR-MS** (ESI-TOF, +eV): *m/z* 1282.4455 (calculated for [M+H]<sup>+</sup>); 1282.4452 (found). Purity by **HPLC** = 90% (R<sub>t</sub> = 23.8 min).

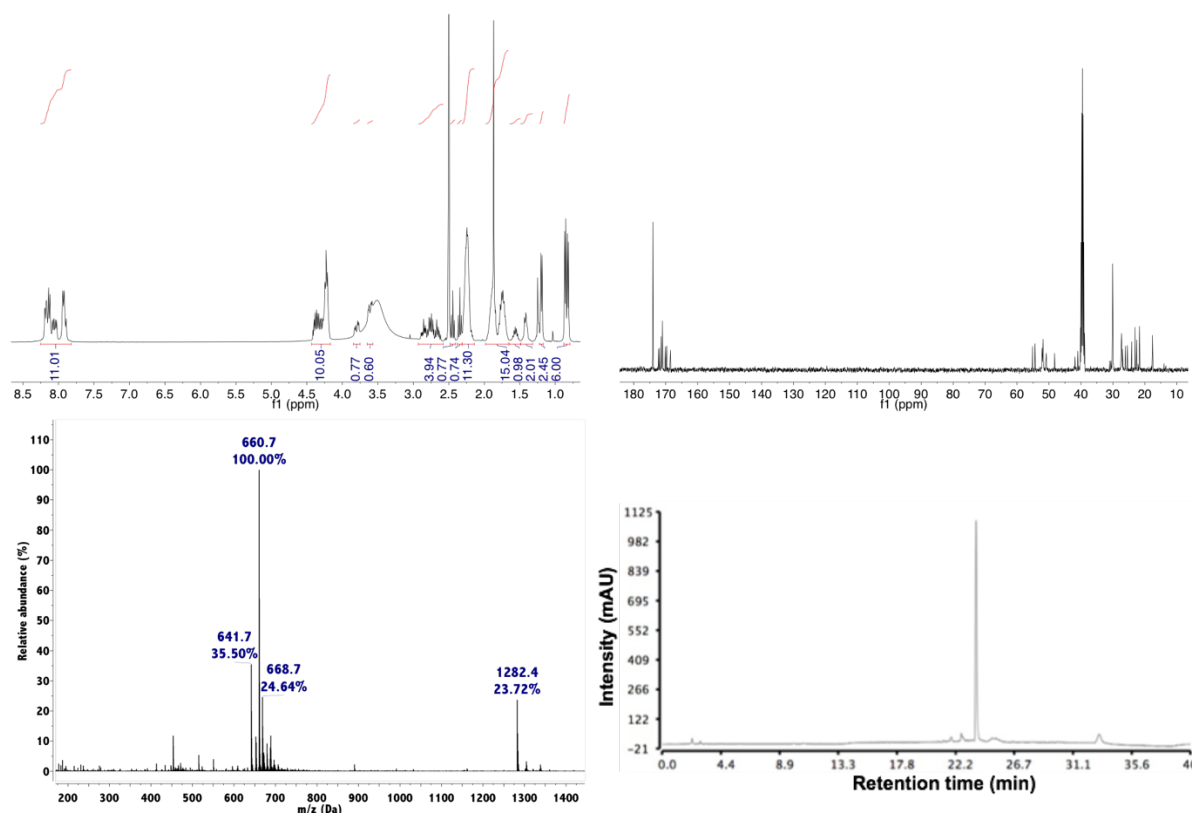
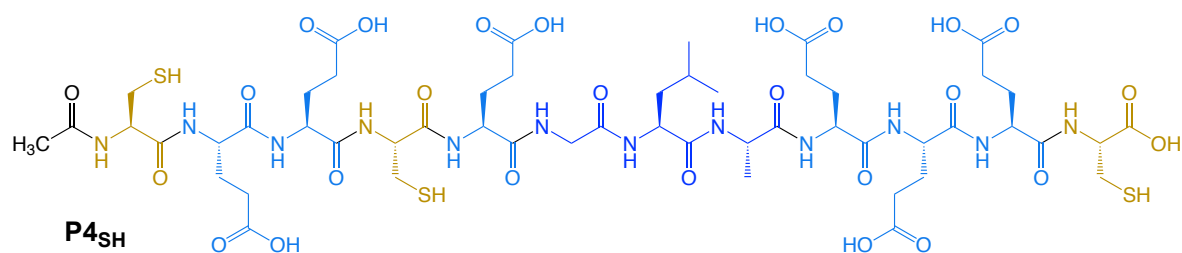


**Figure S2** Characterisation of peptide **P3<sub>SH</sub>** (Ac-C-EEE-GLA-EEE-C-OH). Top: <sup>1</sup>H (left) and <sup>13</sup>C (right) NMR spectra (400 MHz, DMSO-*d*<sub>6</sub>). Bottom: Mass spectrum (left) and RP-HPLC chromatogram (right).



**P4<sub>SH</sub>, Ac-CEECEGLAEEEC-OH** (208.0 mg, 98% yield) **<sup>1</sup>H-NMR** (400 MHz, DMSO-*d*<sub>6</sub>): δ 0.84(dd, *J*=14.5, 6.6 Hz, 6H, H<sup>δ</sup>-Leu); 1.19(d, *J*=7.0 Hz, 3H, H<sup>β</sup>-Ala); 1.36-1.46(m, 2H, H<sup>β</sup>-Leu); 1.51-1.61(m, 1H, H<sup>γ</sup>-Leu); 1.67-1.81(m, 6H, H<sup>β</sup>-Glu); 1.83-1.95(m, 6H, H<sup>β</sup>-Glu); 1.87(s, 3H, Ac); 2.17-2.31(m, 12H, H<sup>γ</sup>-Glu); 2.36(dt, *J*=8.5, 2.8 Hz, 2H, SH); 2.44(t, *J*=8.5 Hz, 1H, SH); 2.62-2.89(m, 6H, H<sup>β</sup>-Cys); 3.70(ddd, *J*=54.5, 16.7, 5.8 Hz, 2H, H<sup>α</sup>-Gly); 4.19-4.42(m, 11H, H<sup>α</sup>); 7.90-8.20(m, 12H, NHCO); 12.16(br.s, 5H, COOH) ppm. **<sup>13</sup>C-NMR** (400 MHz, DMSO-*d*<sub>6</sub>): δ 17.4(C<sup>β</sup>-Ala); 21.4(H<sup>δ</sup>-Leu); 22.3(Ac); 22.9(H<sup>δ</sup>-Leu); 23.9(H<sup>γ</sup>-Leu); 25.2(C<sup>β</sup>-Cys); 25.9(C<sup>β</sup>-Cys); 26.8(C<sup>β</sup>-Cys); 27.0(C<sup>β</sup>-Glu); 27.1(C<sup>β</sup>-Glu); 27.1(C<sup>β</sup>-Glu); 27.2(C<sup>β</sup>-Glu); 40.8(C<sup>β</sup>-Leu); 41.6(C<sup>α</sup>-Gly); 48.0(C<sup>α</sup>); 50.5(C<sup>α</sup>); 51.5(C<sup>α</sup>); 51.6(C<sup>α</sup>); 51.7(C<sup>α</sup>); 51.9(C<sup>α</sup>); 52.1(C<sup>α</sup>); 54.2(C<sup>α</sup>); 54.8(C<sup>α</sup>); 54.9(C<sup>α</sup>); 168.4(NHCO); 169.7(Ac); 170.1(NHCO); 171.0(NHCO); 171.0(NHCO); 171.1(NHCO); 171.1(NHCO); 171.2(NHCO); 171.3(NHCO); 171.4(NHCO); 171.9(NHCO); 172.2(NHCO); 174.0(COOH) ppm. **MS** (ESI-TOF, +eV): *m/z* 1407.4 [M+Na]<sup>+</sup>; 1385.5 [M+H]<sup>+</sup>; 712.2 [M+Ca]<sup>2+</sup>; 704.2 [M+H+Na]<sup>2+</sup>; 693.2 [M+2H]<sup>2+</sup>. **HR-MS** (ESI-TOF, +eV): *m/z* 1385.4547 (calculated for [M+H]<sup>+</sup>); 1385.4545 (found). Purity by **HPLC** = 91% (R<sub>t</sub> = 26.6 min).

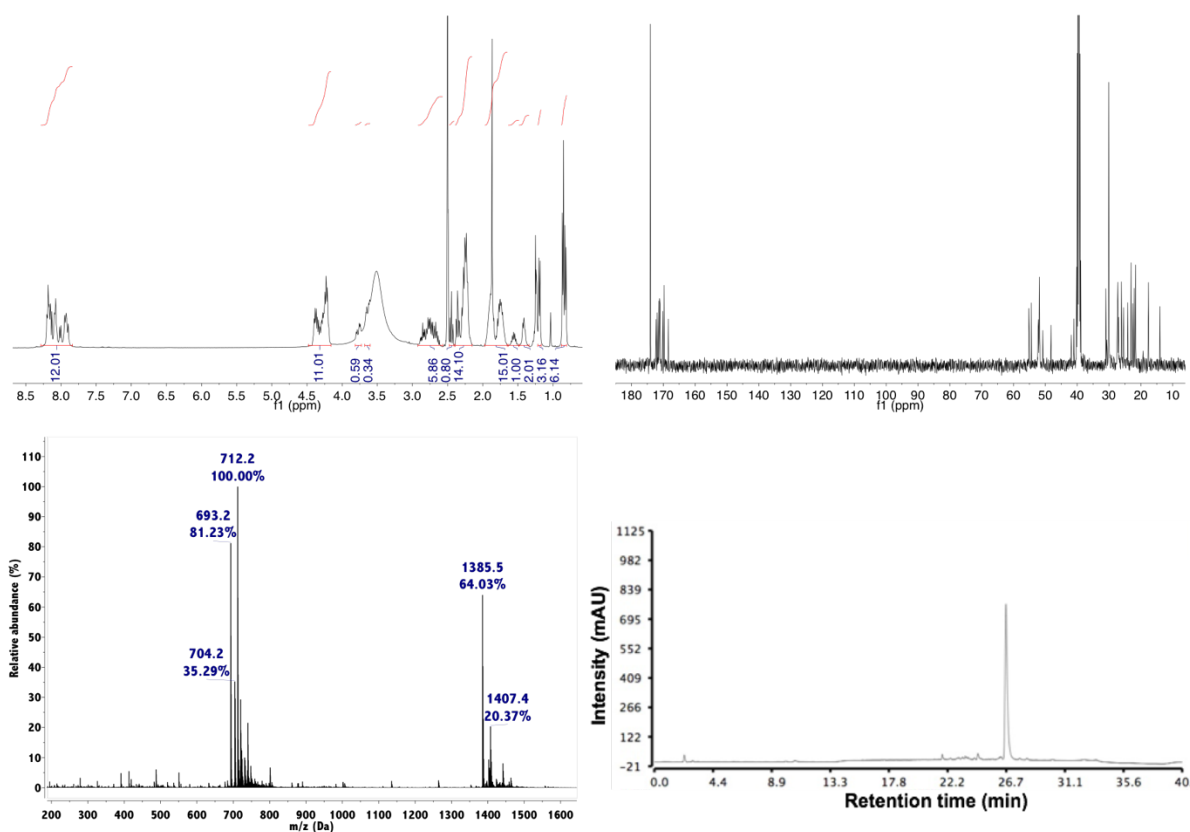


**Figure S3** Characterisation of peptide **P4<sub>SH</sub>** (Ac-C-EE-C-E-GLA-EEE-C-OH). Top: <sup>1</sup>H (left) and <sup>13</sup>C (right) NMR spectra (400 MHz, DMSO-*d*<sub>6</sub>). Bottom: Mass spectrum (left) and RP-HPLC chromatogram (right).

## 5. Enzymatic degradation of peptides

In this experiment several controls have been performed to ensure that the observed increase in fluorescence is related to the elastase-mediated hydrolysis of the peptides.

- Succinyl casein (SC) is a positive control for enzymatic activity. This protein is degraded by most proteases, and an increase in fluorescence for SC in the presence of elastases indicates that these enzymes are active.
- All substrates (e.g. peptide, SC) have been incubated for 4 h under assay conditions in the absence of the elastases and the fluorescence observed is represented by black bars. This includes buffer alone (black bar now labelled control).
- **P5**, a peptide with a sequence that matches the hydrolysis product of one of our previously reported peptides,<sup>[4]</sup> was incubated in the absence of elastase and the fluorescence obtained was associated to 100% hydrolysis.

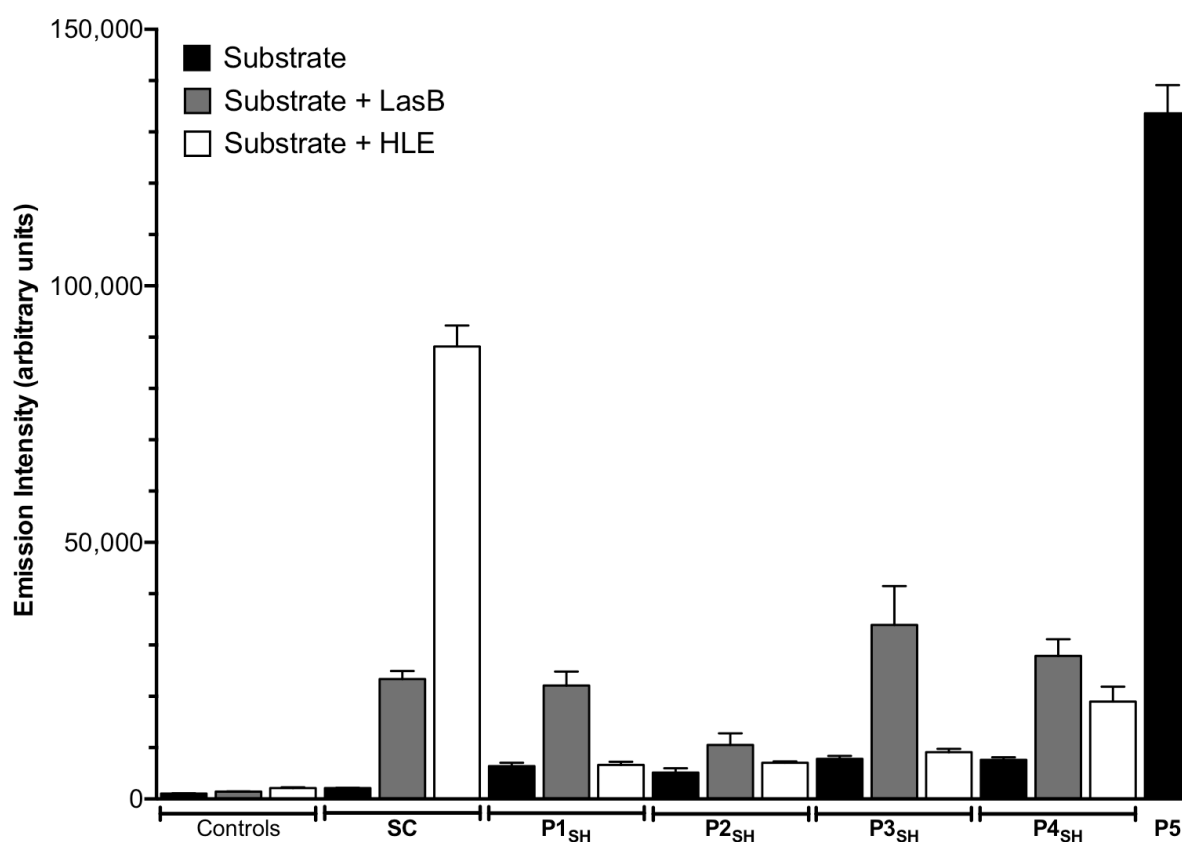


**Figure S4** Emission intensity ( $\lambda_{\text{exc}}$  355 nm,  $\lambda_{\text{em}}$  460 nm) of fluorescamine conjugates for buffer and enzymes (controls), succinyl casein (SC, a control for enzymatic activity) in the absence and presence of enzymes, peptides **P1-4<sub>SH</sub>** in the absence and presence of enzymes, and the peptide H<sub>2</sub>N-LA-E-OH (**P5**, a control to normalise fluorescence intensity). All samples were incubated for 4 hours.  $n = 3$ , mean  $\pm$  SD.

## 6. Circular dichroism characterisation of peptides

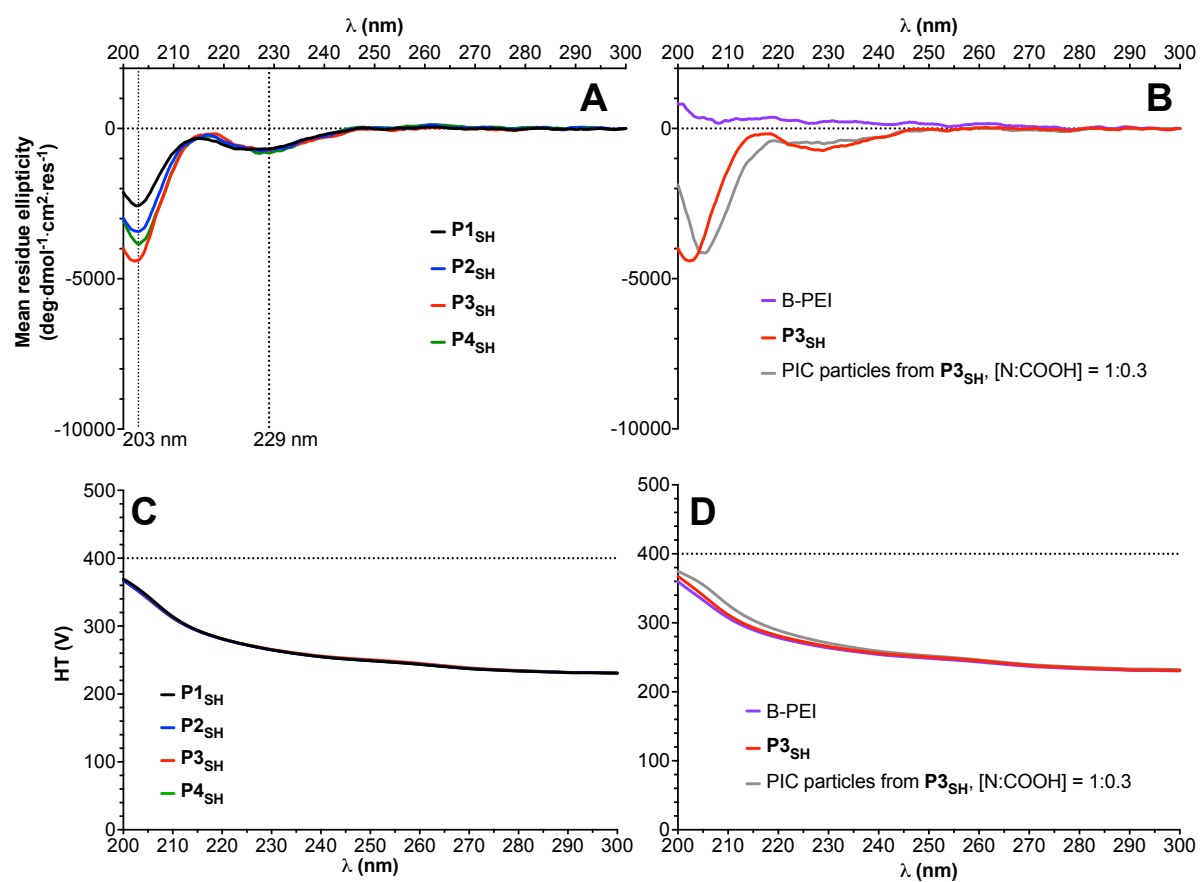


**Figure S5** Top: Circular dichroism absorption spectra of peptides **P1-P4<sub>SH</sub>** (A), and comparison between the spectra of **P3<sub>SH</sub>**, B-PEI and PIC particles prepared from these two materials at a 1:0.3 [N:COOH] ratio (B). Bottom: Dynode (HT) voltages recorded for the spectra above (C-D).

## 7. PIC particle characterisation

**Table S1** Hydrodynamic diameter ( $D_H$ ), polydispersity index (PDI) and  $\zeta$ -potential of PIC particles prepared from peptides **P2-4<sub>SH</sub>** and B-PEI at different [N:COOH] ratios. SD indicates the standard deviation found for the only size or charge population fitted by the software.

Peptide	[N:COOH] ratio	$D_H \pm SD$ (nm)	PDI <sup>a</sup>	$\zeta$ -potential $\pm SD$ (mV)	Notes
<b>P2<sub>SH</sub></b>	1 : 2.0	371 $\pm$ 51	0.02	-9.6 $\pm$ 3.9	-
	1 : 1.5	329 $\pm$ 42	0.02	-10.0 $\pm$ 3.1	-
	1 : 1.0	293 $\pm$ 30	0.01	-9.1 $\pm$ 3.5	-
	1 : 0.8	-	-	-	No particles found
	1 : 0.7	-	-	-	No particles found
	1 : 0.6	-	-	-	No particles found
	1 : 0.5	-	-	-	No particles found
	1 : 0.4	419 $\pm$ 67	0.03	+11.7 $\pm$ 5.2	-
	1 : 0.3	91 $\pm$ 32	0.12	+19.1 $\pm$ 6.2	-
	1 : 0.2	-	-	-	No particles found
<b>P3<sub>SH</sub></b>	1 : 2.0	227 $\pm$ 50	0.05	-21.3 $\pm$ 6.3	-
	1 : 1.5	204 $\pm$ 51	0.06	-18.5 $\pm$ 6.4	-
	1 : 1.0	198 $\pm$ 47	0.06	-18.3 $\pm$ 6.7	-
	1 : 0.8	212 $\pm$ 44	0.04	-16.5 $\pm$ 6.0	-
	1 : 0.7	224 $\pm$ 45	0.04	-16.0 $\pm$ 6.8	-
	1 : 0.6	280 $\pm$ 55	0.04	-15.8 $\pm$ 4.8	-
	1 : 0.5	-	-	-	No particles found
	1 : 0.4	240 $\pm$ 47	0.04	+13.9 $\pm$ 5.1	-
	1 : 0.3	103 $\pm$ 42	0.17	+21.3 $\pm$ 7.9	-
	1 : 0.2	-	-	-	No particles found
<b>P4<sub>SH</sub></b>	1 : 2.0	198 $\pm$ 45	0.05	-20.6 $\pm$ 6.1	-
	1 : 1.5	192 $\pm$ 43	0.05	-20.6 $\pm$ 7.2	-
	1 : 1.0	191 $\pm$ 41	0.05	-20.2 $\pm$ 5.8	-
	1 : 0.8	173 $\pm$ 36	0.04	-17.0 $\pm$ 7.4	-
	1 : 0.7	176 $\pm$ 39	0.05	-17.7 $\pm$ 7.2	-
	1 : 0.6	205 $\pm$ 39	0.04	-11.1 $\pm$ 7.5	-
	1 : 0.5	-	-	-	No particles found
	1 : 0.4	225 $\pm$ 46	0.04	+15.2 $\pm$ 5.4	-
	1 : 0.3	143 $\pm$ 40	0.08	+17.7 $\pm$ 7.7	-
	1 : 0.2	-	-	-	No particles found

The size and charge of PIC nanoparticle formulations prepared from peptide **P1<sub>SH</sub>** has been previously reported.<sup>[3]</sup> <sup>a</sup> PDI values were calculated from the  $D_H$  and SD obtained by *General Purpose* (Malvern Instruments Ltd.) deconvolution of DLS correlograms using the following formula:  $PDI = (SD/D_H)^2$ .<sup>[5]</sup>



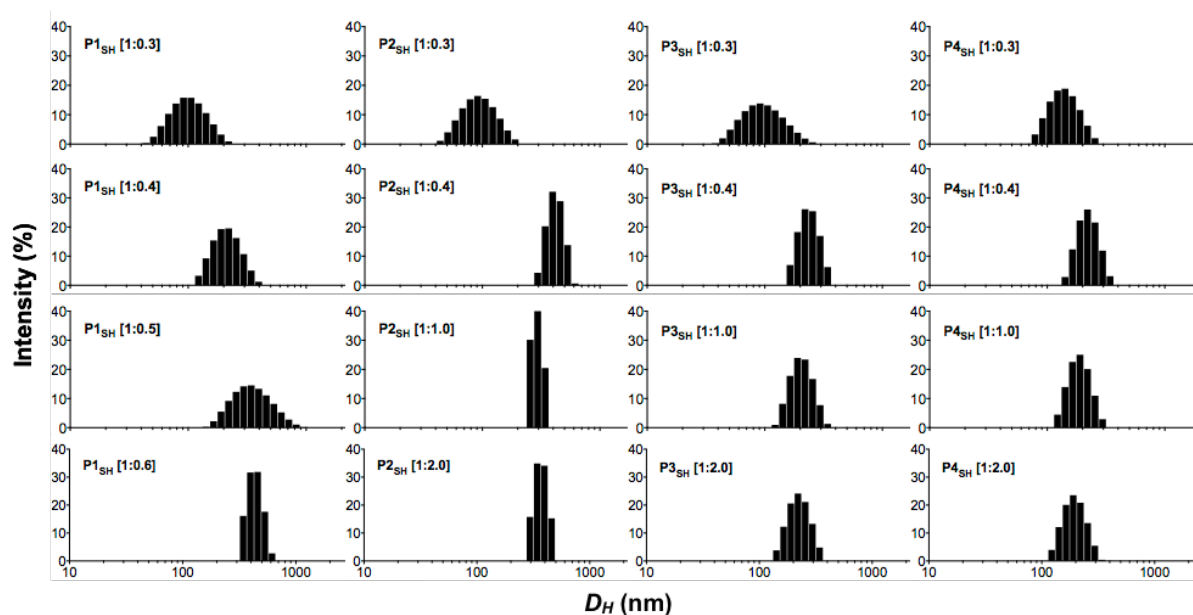


**Figure S6** Representative DLS size-intensity distributions of freshly prepared PIC nanoparticles containing peptides **P1<sub>SH</sub>**-**P4<sub>SH</sub>** at different N:COOH ratios.

#### 8. SLS characterisation of unfiltered PIC particles

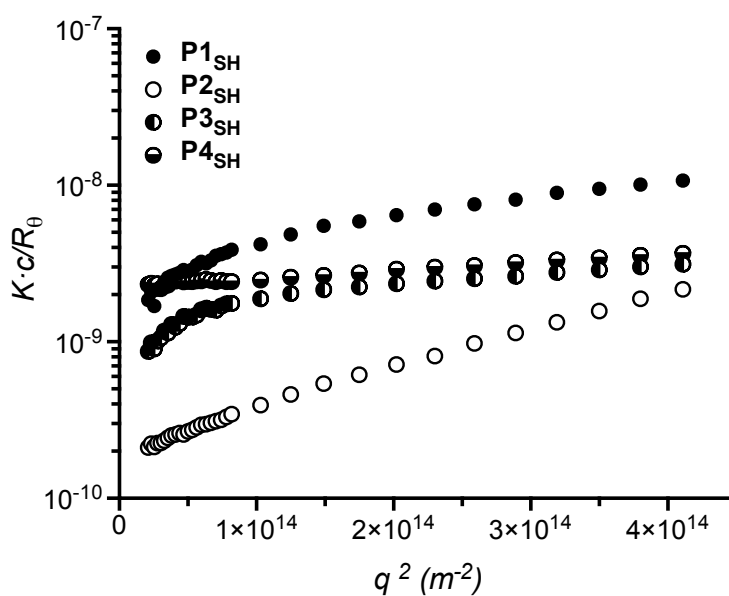


**Figure S7** Partial Zimm plots obtained by SLS of unfiltered PIC particles prepared from peptides **P1-4<sub>SH</sub>** at a 1:0.3 [N:COOH] ratio.

## 9. Shelf stability of PIC particles

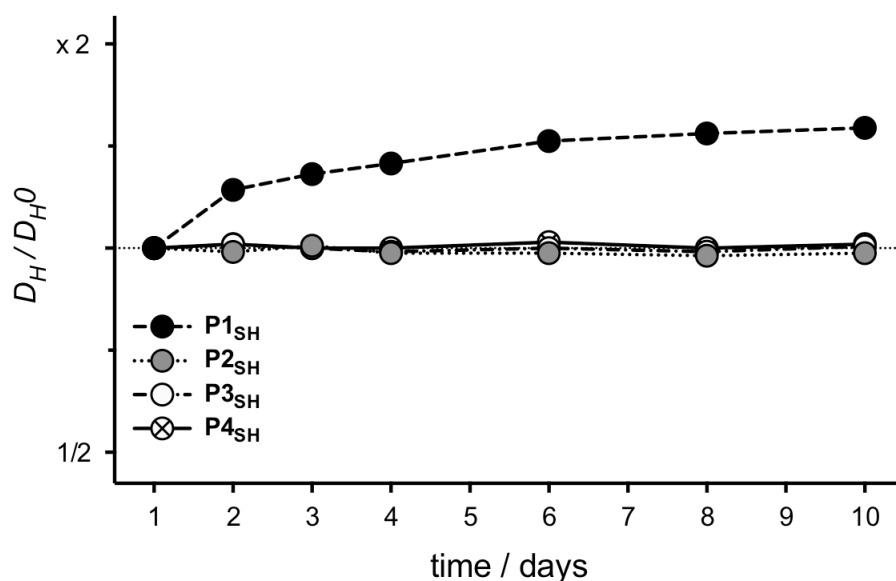


**Figure S8** Relative change in size ( $D_H / D_{H0}$ ) over time of PIC particles prepared at a 1:0.3 [N:COOH] ratio, stored in a dark, cool and dry place. The  $D_H$  values calculated by DLS were normalised to that of freshly made PIC particles (day 1).

## 10. Stability of the particles under physiological conditions

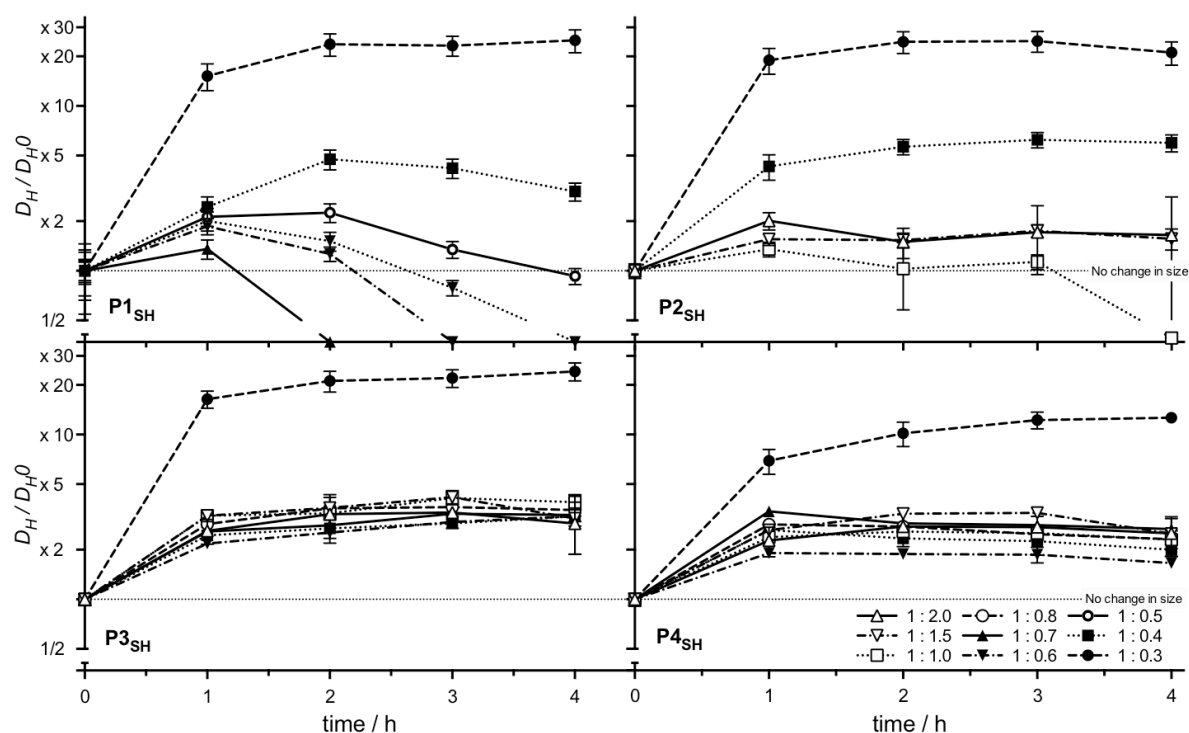


**Figure S9** Relative change in size ( $D_H / D_{H0}$ ) for PIC particles prepared from peptides P1<sub>SH</sub>-P4<sub>SH</sub> at representative N:COOH ratios under simulated physiological conditions (37 °C, 154 mM NaCl, pH 7.4). Particle size ( $D_H$ ) were normalised to that of the PIC particles in the absence of NaCl (0 hours, No change in size).  $n = 3$ , mean values  $\pm$  standard deviation. Results obtained directly after the assembly of the nanoparticles without prior filtration. Data for P1<sub>SH</sub> reproduced from I. Insua, E. Lamas, Z. Zhang, A. F. Peacock, A. M. Krachler, F. Fernandez-Trillo, *Polym Chem* **2016**, 7, 2684–2690 - Published by The Royal Society of Chemistry.

**11. Additional references**

- [1] N. J. Greenfield, *Nat. Protoc.* **2006**, 1, 2876–2890.
- [2] T. Vojkovsky, *Pept. Res.* **1995**, 8, 236–237.
- [3] I. Insua, E. Lamas, Z. Zhang, A. F. A. Peacock, A. M. Krachler, F. Fernández-Trillo, *Polym. Chem.* **2016**, 7, 2684–2690.
- [4] K. Morihara, H. Tsuzuki, *Arch. Biochem. Biophys.* **1971**, 146, 291–296.
- [5] Malvern Instruments Ltd., *Application of Dynamic Light Scattering (DLS) to Protein Therapeutic Formulations: Principles, Measurements and Analysis - 3. DLS Deconvolution Algorithms*, **2014**.